Simulation of proton–boron nuclear burning in the potential well of virtual cathode at nanosecond vacuum discharge

Yu K Kurilenkov[1], V P Tarakanov[1,3] and S Yu Gus'kov[1,2,3]

[1] Joint Institute for High Temperatures of the Russian Academy of Sciences, Izhorskaya 13 Bldg 2, Moscow 125412, Russia
[2] Lebedev Physical Institute of the Russian Academy of Sciences, Leninsky Avenue 53, Moscow 119991, Russia
[3] National Research Nuclear University MEPhI (Moscow Engineering Physics Institute), Kashirskoe Shosse 31, Moscow 115409, Russia

E-mail: kurilenkovyuri@gmail.com

Abstract. The neutron-free reaction of proton–boron nuclear burning accompanied with the yield of three alpha particles ($p + {}^{11}B \to \alpha + {}^{8}Be^{*} \to 3\alpha$) is of great fundamental and applied interest. However, the implementation of the synthesis of $p + {}^{11}B$ requires such extreme plasma parameters that are difficult to achieve at well-known schemes of controlled thermonuclear fusion. Earlier, the yield of DD neutrons in a compact nanosecond vacuum discharge (NVD) of low energy with deuterated Pd anode have been observed. Further detailed particle-in-cell simulation by the electrodynamic code have recognized that this experiment represents the realization of rather old scheme of inertial electrostatic confinement (IEC). This IEC scheme is one of the few where the energies of ions needed for $p + {}^{11}B$ reaction are quite possible. The purpose of this work on simulation of proton–boron reaction is studying the features of possible $p + {}^{11}B$ burning at the IEC scheme based on NVD, thus, to look forward and planning the real experiment.

1. Introduction

The neutron-free reaction of proton–boron nuclear burning accompanied with the yield of three alpha particles ($p + {}^{11}B \to \alpha + {}^{8}Be^{*} \to 3\alpha$) is of great fundamental and applied interest (radioactive elements are also practically absent here) [1–7]. Controlled fusion reactions between protons and boron-11 nuclei would mean, in particular, the principal possibility of establishing of a transforming source of electricity, possessing advantages over the known sources of energy. Since the energy output is carried out in this scheme exclusively due to the charged particles, in principle, it enables the direct conversion of the kinetic energy of the alpha particles into electricity [4, 7]. However, as is well known (see, for example, [1, 4, 7]), the implementation of the synthesis of $p + {}^{11}B$ requires such extreme plasma parameters that are difficult to achieve. Nevertheless, attempts to achieve the required parameters occurs, and interest in the problem of proton–boron burning is growing permanently [2–11]. The first experiment on laser-driven proton–boron burning have used a composite target and gave an alpha particle yield per laser pulse about $\sim 10^3$ per steradian [8]. Much higher alpha-particle yield $\sim 10^7$ have been registered under colliding of laser-accelerated proton beam with a laser-generated boron plasma [9]. Also,

Content from this work may be used under the terms of the Creative Commons Attribution 3.0 licence. Any further distribution of this work must maintain attribution to the author(s) and the title of the work, journal citation and DOI.
Published under licence by IOP Publishing Ltd

even higher alpha-particle yield (up to $\sim 10^9$) have been obtained under boron-proton fusion induced in boron-doped silicon target by low contrast nanosecond laser [10]. The conditions needed for aneutronic fusion like p + ^{11}B have been achieved using a dense plasma focus device also [11].

Earlier, the yield of DD neutrons in a compact nanosecond vacuum discharge (NVD) of low energy with deuterated Pd anode have been observed [12]. Further, detailed particle-in-cell (PIC) simulation by the electrodynamic code KARAT have recognized [13] that experiment with NVD have represented the realization of rather well-known scheme of inertial electrostatic confinement (IEC) [4, 7, 14, 15]. The purpose of this work on modeling of proton-boron burning is studying the features of possible reaction p + ^{11}B at the scheme of IEC based on NVD [12,13,15,16]. Since KARAT code PIC modeling have described properly the experimental results on DD fusion at NVD earlier [13, 15], now we supposed to rely upon on this simulation data on p + ^{11}B burning at NVD to look forward and planning the real experiment.

2. PIC simulation of p + ^{11}B burning at nanosecond vacuum discharge with IEC

The present PIC simulation of p+ ^{11}B burning at NVD by KARAT code [17] is carried out in the axially symmetric approximation (see preliminary modeling data in [15]). In whole and briefly, the voltage pulse with leading front of 0.1 ns and amplitude of 150 kV is applied to the diode gap along the coaxial. Then evolutions of the voltage at the coaxial inlet and the voltage between the anode and the virtual cathode (VC) are calculated. On the part of the cathode surface there is provided self-consistent emission of electrons. The latter, while passing of electrons through the "translucent" anode modeled as a foil creates plasma. Then electrons continue their movement towards the axis, where they are forming the virtual cathode [16]. Boron ions and protons accelerate from the anode foil in the potential well (PW) of the virtual cathode in the direction of the axis, where their density and energy of head-on collisions are increasing, which actually leads to the appearance of alpha particles [15]. For the calculations there is used a block, in which fusion reaction p+ ^{11}B is simulated, besides, a separate block of ^{8}Be* decay is used at that. An example of simulation of discharge in the KARAT code at the discharge parameters close to current actual operating ones (U = 150 kV, I = 1–2 kA) is represented and discussed in detail below in figures 1–5.

In the considered design (figure 1a), a positive voltage is applied to the center electrode (anode) saturated with materials, which nuclei may enter into interesting for modeling a nuclear reaction, in this case p + B^{11} $\rightarrow$ ^{8}Be* + He^4 and following disintegration of nuclei ^{8}Be* $\rightarrow$ He^4 + He^4. The outer cylindrical electrode (cathode) under the ground potential there is the emitter of an electron current reaching some kAmps. The electron flow passes through the partially transparent anode and nearby of axis forms a negatively charged region (figure 1a) that under certain conditions with a potential close to ground potential, i.e. the virtual cathode is formed. Saturated anode materials (green area, figure 1a) exposed to the flow of electrons, emits ions and protons, which are under the influence of the virtual cathode field begin to move towards the axis (figure 1b), in the vicinity of which are gaining sufficient energy for p + ^{11}B nuclear reactions. Unreacted ions continue to move, which comes down to oscillations in a region restricted by anode (figure 4a). At each passage of the axial region of the part of ions entering the nuclear reaction. Due to the finite size along the axis, the collisions and the anode heterogeneity, consisting now of a few tubes, the ions gradually leave the central region and the process is damping.

To simulate the described processes in the framework of an axially symmetric model, the fully electromagnetic relativistic PIC code KARAT have been used. Simulation region shown in figure 1a) was built, where the blue line corresponds to the outer grounded cathode, of the red line to the anode the central part of which is saturated by materials for nuclear reactions. An ionization process they are not seen, and at the initial time in the area of the anode is loaded

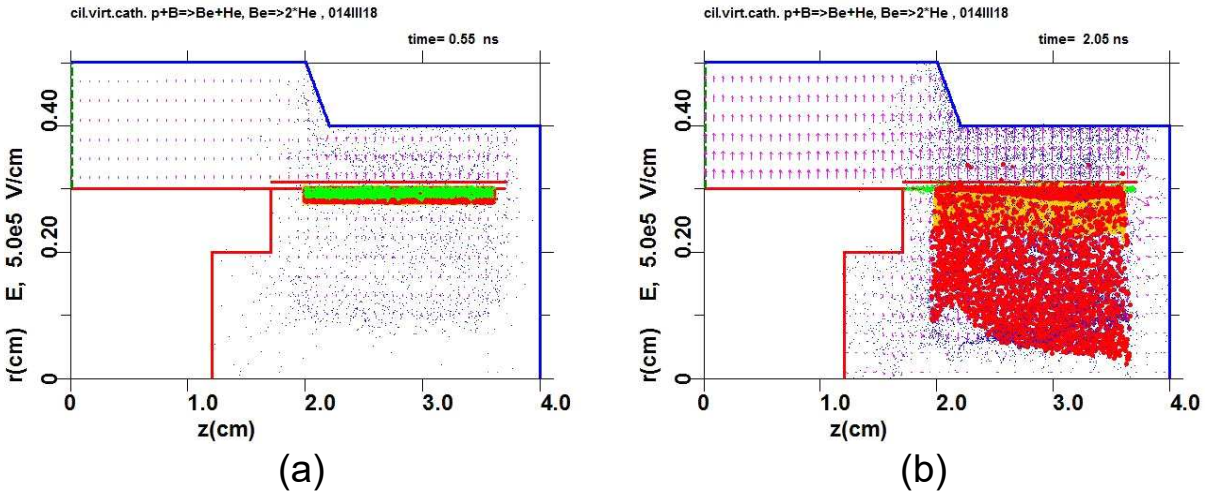

Figure 1. (a) Anode (red)–cathode (blue) geometry in discharge gap of NVD where the virtual cathode is formed (at 0.55 ns); green area-simulated "erosion plasma" consisting of protons and boron ions. (b) The start of moving of protons (red ones) and boron ions (yellow) at potential well of virtual cathode to axis Z where p+ ^{11}B reaction will take place (this picture corresponds to 2.05 ns of simulation).

with clouds of neutral plasma consisting of electrons, protons and ions of triply ionized boron (figure 1a). The degree of ionization is selected here on the assumption that the atom ^{11}B loses of the outer electrons. In general, the anode plasma density is variable parameter. In the present modeling it is chosen equal to 10^{13} cm^{-3} that corresponds to very low initial density nearby of anode surface irradiated by electron flux from cathode. The voltage across the gap increases to 100–150 kV, which corresponds to the parameters of the experiment modified with NVD [15,16]. Geometrical transparency of anode is chosen equal to 90%. PIC particles if reaching any surface are absorbing.

The code KARAT solves the complete system of Maxwell's equations, for which the current density is calculated by PIC method based on the dynamics of macro particles in self-consistent electromagnetic fields. To simulate all types of particles of actual process p + ^{11}B $\rightarrow \alpha +$ ^{8}Be* $\rightarrow 3\alpha$ the several types of PIC particles are used, namely: blue PIC particles—emitted electrons, green ones—anode plasma electrons, red ones—protons, $Z = +1$; yellow ones—11B, $Z = +3$; gray ones—^{8}Be*, $Z = +2$; violet ones—He^{4}, $Z = +2$—reaction product (primary alpha-particles); dark orange ones—He^{4}, $Z = +1$—product of ^{8}Be* disintegration (secondary alpha-particles). In the process of simulation in a special unit at each time step, and for each PIC particle is calculated the probability of a nuclear reaction p + ^{11}B $\rightarrow$ ^{8}Be* + He^{4} + 3.27 MeV, using the cross sections of this process [18–20]. Then, for the generated ions ^{8}Be* the probability of decay ^{8}Be* $\rightarrow$ He^{4} + He^{4} is calculated with using of experimental values that describes this process [18]. The energy released in nuclear reactions divides between the particles in accordance with the momentum conservation law. All generated particles acquired the corresponding momentum continue to move in electromagnetic fields, creating corresponding currents in the simulation region. Remark, in general case at simulation for fully ionized boron ions with $Z = +5$ we will get the correct value $Z = +2$ for secondary alpha-particles certainly.

Let us consider in more detail a number of the pictures describing the studied process. In figure 1a (1 ns) it is visible how electrons (blue particles) are emitted from an external electrode, passing through the anode and going to the axial region where are braked by the field of VC. Then they are reflected and are scattering partially. Positive particles of anode plasma (red —

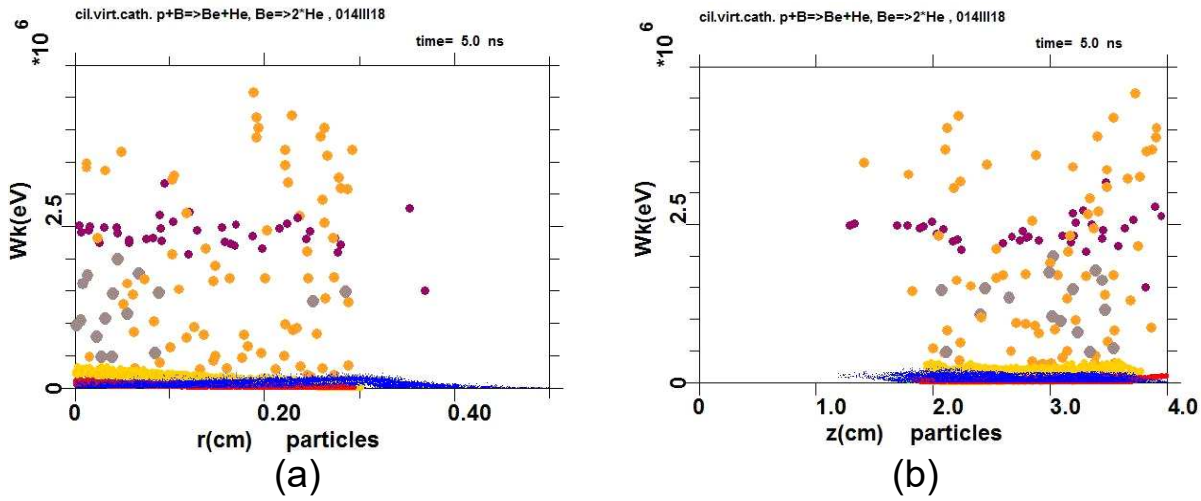

Figure 2. (a) Energy of all particles participating in a nuclear reaction p + ^{11}B $\rightarrow \alpha +$ ^{8}Be* $\rightarrow$ 3α as a function of their position along the radius (blue points—electrons, yellow—boron ions, red—protons, gray—^{8}Be*, $Z = +2$; violet—He^{4}, $Z = +2$, primary α-particles; dark orange—He^{4}, $Z = +1$—a product of disintegration of ^{8}Be* secondary α-particles). (b) Energy of the same particles as a function of their position along the axis Z.

protons, yellow—boron ions) are draw off by the field of VC towards the axis Z. To the 2nd ns (figure 1b) more light protons have moved closer to an axis than ^{11}B ions. To 5th ns ions have reached the axis Z and nuclear processes are starting that accompanied by the yield of all the products of p + B^{11} reaction. The particular particles yield on 5th ns is presented in figure 2, where the energies and positions in A–C space of NVD for electrons, protons and boron ions as well as for generated products are shown (all particles are listed in figure 2 caption).

In whole, alpha particles spectra obtained under PIC modeling do correspond to well-known experimental and theoretical ones [18–20]. Remark, rather low energies of primary α–particles calculated is due to the low of moment conservation (since ^{8}Be* have certain energy also, figure 2).

The phase portrait of the particles (figure 3a) shows the process of acceleration of electrons nearly up to $V_{r/c} \sim 0.5$, and then their slow-downing almost on the discharge axis with formation of the virtual cathode ($V_{r/c} \sim 0$). The corresponding to VC potential well is shown in figure 3b). Boron ions and protons are drawn by the field from the green area of the anode "erosion plasma" and accelerated in the PW to the discharge axis (figure 3a). Transformation of the energy of the electron beam into the energy of boron ions and protons is well illustrated in figure 2a). It can be seen that the protons, while approaching the axis of the discharge, reach the same maximum energy that the electrons have when approaching the anode grid provided of Pd rods in real experiment [13, 16]. The energy of boron ions in the PW bottom is proportional to their charge $Z = +3$, as shown in figure 2, i.e. it is almost three times higher in relation to the protons.

Momentary position of boron ions and protons will correspond to their oscillating around the axis Z in the PW of VC at anode interior area (figure 4a). The changing in time of the energies of the isolated groups of protons and boron ions in the RZ plane is shown in figure 4b. Probabilities of p + ^{11}B fusion (and alpha-particles bursts related) will be sharply increasing in certain moments of "thickening" of the trajectories of protons and boron ions (for maximum energies of individual groups during the collapse of the particles on the bottom of the potential well). Additionally, the time histories of particle throughout the first 20 ns are shown in figure 5a. Secondary α-particles yield arising from beryllium disintegration is presented in

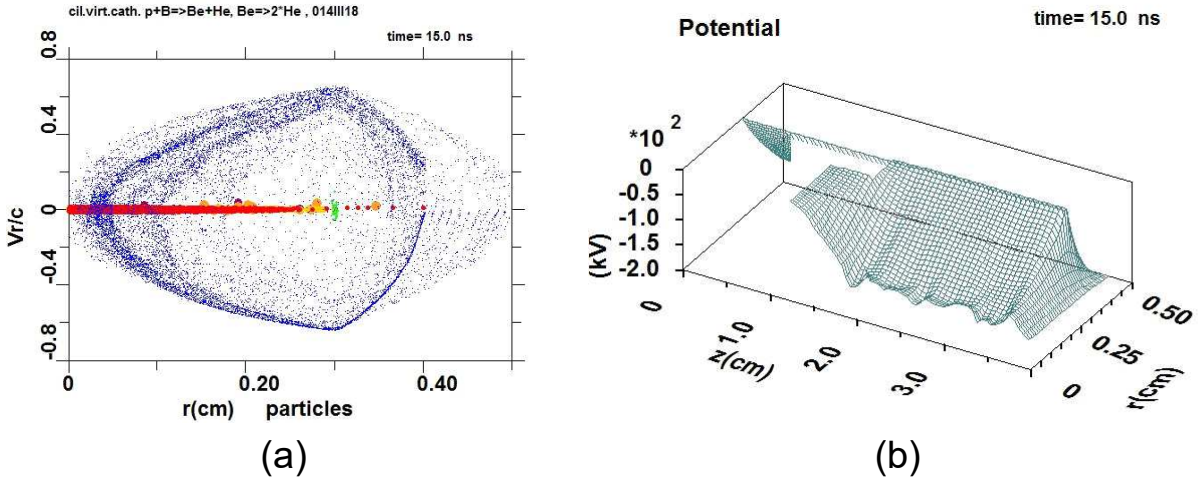

Figure 3. (a) Velocities of all particles as a function of their position along the radius (phase portrait) of the anode–cathode geometry being studied (formation of virtual cathode in the area of $r \leq 0.1$ cm at slow-downing of the electrons is presented, while protons and boron ions are accelerating in the potential well to the discharge axis), all symbols as in figure 2, c–velocity of light. (b) Potential well of the virtual cathode as possible micro-"reactor" for p + ^{11}B nuclear burning at NVD with IEC.

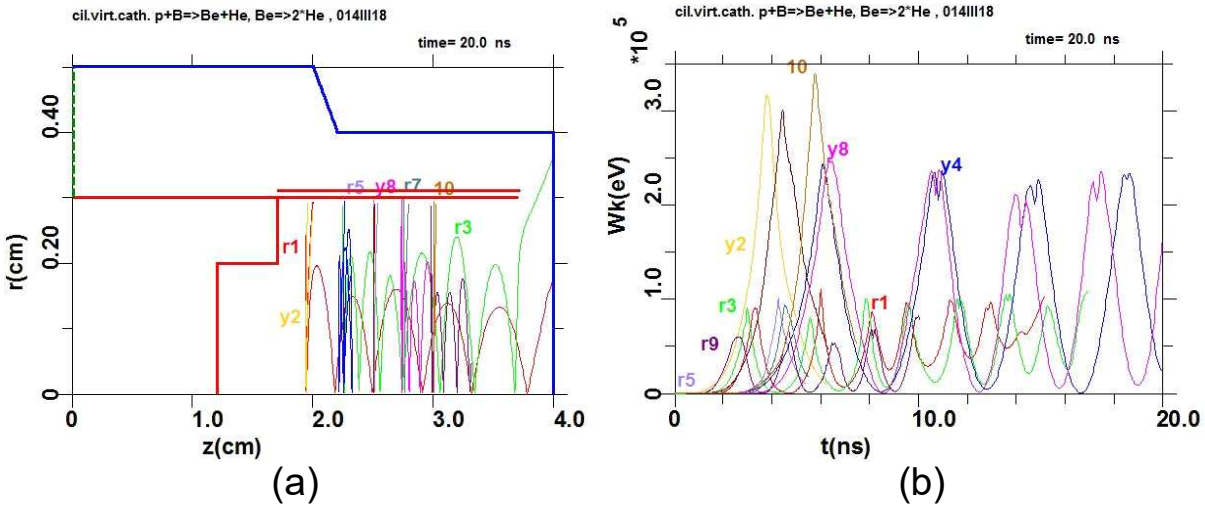

Figure 4. (a) Trajectories of particular groups of boron ions (y, $Z = +3$) and protons (r) during their oscillating around the axis Z at anode space. (b) Energy of chosen groups of protons and boron ions as a function of time in the process of oscillations in potential well (within the interval 0–20 ns).

figure 5b. Primary α-particles yield looks very similar. Remark, qualitatively, the pulsating yield of α-particles in time (figure 5b) reminds burning waves in proton-boron plasmas mentioned for other conditions earlier [21].

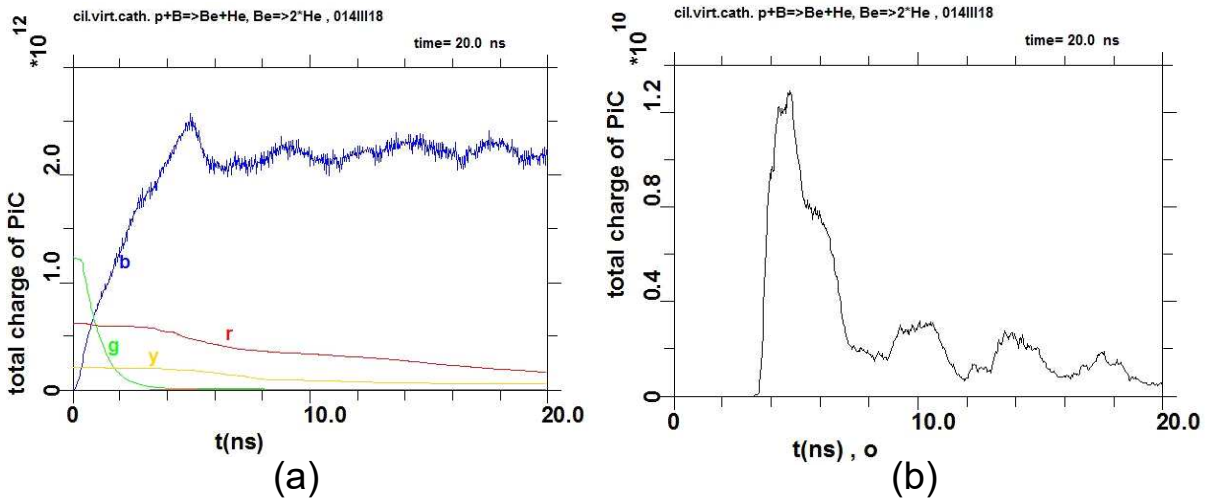

Figure 5. (a) The time histories of particle total number throughout the first 20 ns (b—electrons of beam, g—anode plasma density, r—protons, y—boron ions). (b) An example of secondary alpha-particles yield from disintegration of ^{8}Be*.

3. Concluding remarks

The purpose of this simulation was to determine some specifics of the synthesis reaction in the interaction of the nuclei of ^{11}B with protons in NVD type of IEC device containing the discharge gap of a few mm with a typical voltage of $\sim 10^5$ V (the rise time order of 0.1 ns was chosen for better "keeping" of anode "erosion plasma" before reaction starting in simulation). It should be reminded that the cross-section of proton-boron reaction is changing almost by thirteen orders of magnitude when the temperature of the ions in the plasma changes from 10 keV to 100 keV [1]. In the future experiment we will be interested in the area in the vicinity of the narrow peak of p + ^{11}B reaction cross-section at an energy of 148 keV [1], which is achievable in the obtained PW (figure 4b) even for single charged boron ions. Remark, the well-known schemes of controlled thermonuclear fusion [1, 2] do not allow achieving such temperatures, while the scheme with IEC is one of the few where such energies of ions are quite possible. Moreover, energy losses to Bremsstrahlung radiation under thermal equilibrium fusion burn if available would prevent this reaction from being self-sustaining. Such problems could be overcome by driving the p + ^{11}B reaction under conditions far from equilibrium and IEC scheme do provide it [4, 7, 15, 22] as well as some of laser-driven fusion schemes [9, 10, 23, 24]. That is why the presented modeling of p + B^{11} burning at IEC based on NVD looks reasonable, meanwhile, the PIC simulated spectra of all particles in the reaction p + ^{11}B $\rightarrow \alpha +$ ^{8}Be$^* \rightarrow 3\alpha$ (like in figure 2) do represent the special interest. Current PIC modeling have recognizing that transfer to almost pure cylindrical geometry of cathode allows to optimize some of the key parameters of nuclear burning at PW of VC in NVD, for example, the shape and the deepness of PW, and probably will allow to find the proper ways to increase the efficiency of p + B^{11} reaction at the future experiment. This operating example illustrates only the possibilities of using the KARAT code to describe and optimize the p + B^{11} synthesis conditions in the potential well of the NVD. The presented results allow us to be oriented in the processes of possible burning p + ^{11}B in NVD, but they are still rather far from the optimum. The efficiency of p + ^{11}B reactions, the quantitative α-particles yield in NVD, 3D effects in PIC simulations, possible an avalanche increase of the reaction yield [6, 25–27] and looking for $Q > 1$ [28] are the subjects of further study and simulation.

Acknowledgments
This work was supported by the Russian Science Foundation (grant No. 14-50-00124).

References
[1] Atzeni S and Meyer-ter-Vehn J 2004 *The Physics of Inertial Fusion* (Oxford, UK: Oxford Univ. Press)
[2] Moreau D C 1977 *Nucl. Fusion* **17** 13–20
[3] Rostoker N, Binderbauer M W and Monkhorst H J 1997 *Science* **278** 1419–1422
[4] Kulcinski G L and Santarius J F 1998 *Nature* **396** 724–725
[5] Nevins W M and Swain R 2000 *Nucl. Fusion* **40** 865–872
[6] Hora H, Korn G, Giuffrida L, Margarone D, Picciotto A, Krasa J, Jungwirth K, Ullschmied J, Lalousis P, Eliezer S, Miley G H, Moustaizis S and Mourou G 2015 *Laser Part. Beams* **33** 1–13
[7] Miley G and Murali S K 2014 *Inertial Electrostatic Confinement (IEC) Fusion* (Springer, New York)
[8] Belyaev V S, Matafonov A P, Vinogradov V I, Krainov V P, Lisitsa V S, Roussetski A S, Ignatyev G N and Andrianov V P 2005 *Phys. Rev.* E **72** 026406
[9] Labaune C, Baccou C, Depierreux S, Goyon C, Loisel G, Yahia V and Rafelski J 2013 *Nat. Commun.* **4** 2506
[10] Picciotto A, Margarone D, Velyhan A, Bellutti P, Krasa J, Szydlowsky A, Bertuccio G, Shi Y, Mangione A, Prokupek J, Malinowska A, Krousky E, Ullschmied J, Laska L, Kucharik M and Korn G 2014 *Phys. Rev.* X **4** 031030
[11] Lerner E J, Murali S K, Blake A M, Shannon D M and van Roessel F J 2012 *Nukleonika* **57** 205–209
[12] Kurilenkov Y K, Skowronek M and Dufty J 2006 *J. Phys. A: Math. Gen.* **39** 4375
[13] Kurilenkov Y K, Tarakahov V P, Skowronek M, Gus'kov S Y and Dufty J 2009 *J. Phys. A: Math. Theor.* **42** 214041
[14] Lavrent'ev O A 2012 *On the History of Thermonuclear Synthesis in USSR* (Kharkov: Kharkov Phys.-Tech. Inst.) 2nd ed
[15] Kurilenkov Y K, Tarakahov V P, Karpukhin V T, Gus'kov S Y and Oginov A V 2015 *J. Phys.: Conf. Ser.* **653** 012025
[16] Kurilenkov Y K, Tarakahov V P, Gus'kov S Y, Samoylov I S and Ostashev V E 2015 *J. Phys.: Conf. Ser.* **653** 012026
[17] Tarakanov V P 1992 *User's Manual for Code KARAT* (Va, USA: BRA Inc.)
[18] Becker H W, Rolfs C and Trautvetter H P 1987 *Z. Phys. A: At. Nucl.* **327** 341–355
[19] Stave S, Ahmed M W, France III R H, Henshaw S S, Muller B, Perdue B A, Prior R M, Spraker M C and Weller H R 2011 *Phys. Lett.* B **696** 26–29
[20] Dmitriev V F 2009 *Phys. At. Nucl.* **72** 1165–1167
[21] Martinez-Val J M, Eliezer S, Piera M and Velarde G 1996 *Phys. Lett.* A **216** 142–152
[22] Hirsch R L 2012 *14th U.S.–Japan IECF Workshop*
[23] Khishchenko K V and Charakhch'yan A A 2015 *J. Appl. Mech. Tech. Phys.* **56** 86–95
[24] Krasyuk I K, Pashinin P P, Semenov A Y, Khishchenko K V and Fortov V E 2016 *Laser Phys.* **26** 094001
[25] Eliezer S, Hora H, Korn G, Nissim N and Martinez J M 2016 *Phys. Plasmas* **23** 050704
[26] Belyaev V S, Krainov V P, Zagreev B V and Matafonov A P 2015 *Phys. At. Nucl.* **78** 537–547
[27] Belyaev V S, Krainov V P, Matafonov A P and Zagreev B V 2015 *Laser Phys. Lett.* **12** 096001
[28] Gus'kov S Y and Kurilenkov Y K 2016 Neutron yield and lawson criterion for plasma with inertial electrostatic confinement This issue